

Cognitive dysfunction in early experimental metabolic dysfunction-associated steatotic liver disease is associated with systemic inflammation and neuroinflammation

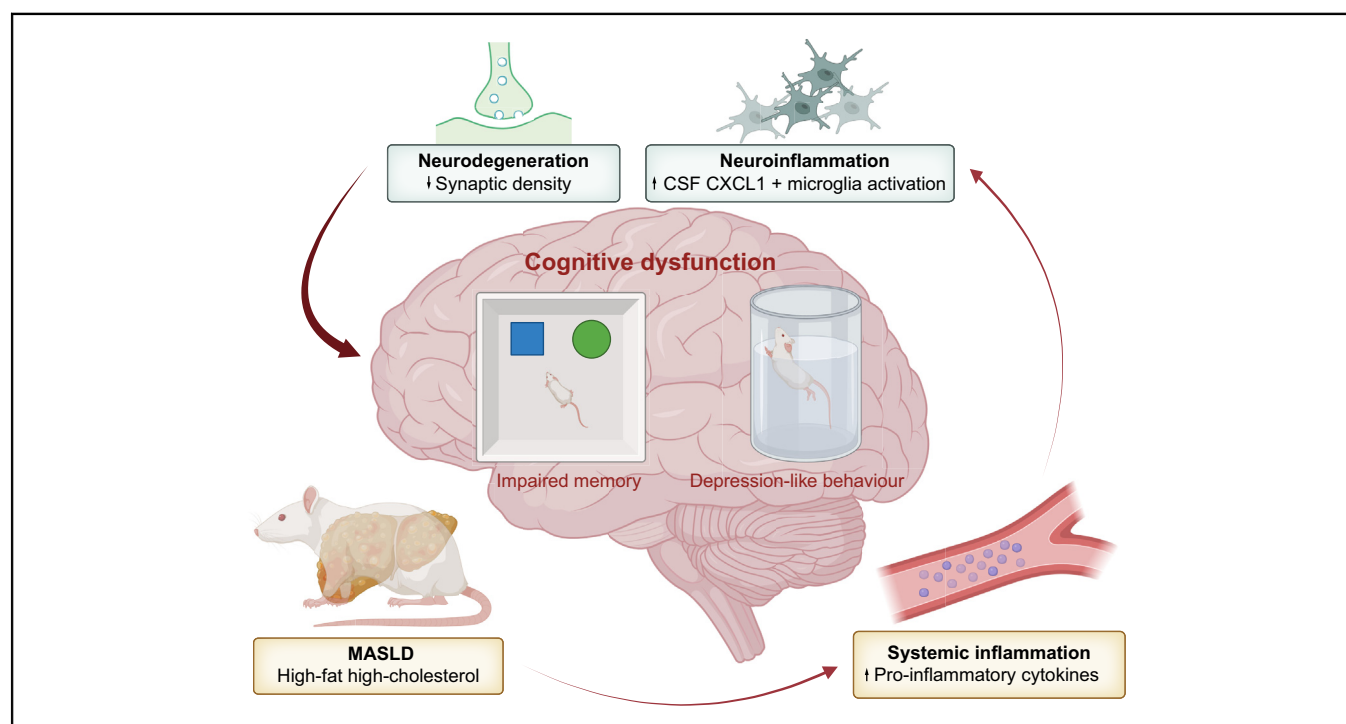
Authors

Kristoffer Kjærgaard, Anne Catrine Daugaard Mikkelsen, Anne M. Landau, Peter Lykke Eriksen, Stephen Hamilton-Dutoit, Nils Erik Magnusson, Majken Borup Thomsen, Fenghua Chen, Hendrik Vilstrup, Rajeshwar Prosad Mookerjee, Cecilie Bay-Richter, Karen Louise Thomsen

Correspondence

karethom@rm.dk (K.L. Thomsen).

Graphical abstract



Highlights

- This study provided evidence of memory loss and altered behavior in a MASLD animal model.
- Cognitive dysfunction was associated with systemic inflammation and neuroinflammation.
- Microglia activation and diminished synaptic density were observed in the prefrontal cortex.
- The study suggests a pathophysiological link between MASLD and cognitive dysfunction.

Impact and implications

Cognitive dysfunction is an increasingly recognised comorbidity in patients with metabolic dysfunction-associated steatotic liver disease (MASLD), yet the underlying mechanisms remain unclear. This study provides evidence of impaired memory and depression-like symptoms in early experimental MASLD and indicates that hepatic inflammation may drive a systemic inflammatory response, resulting in neuroinflammation and reduced brain synaptic density. The evidence of impaired memory in MASLD and establishing its underlying pathophysiological link provides insights that could guide the development of potential new treatments for this increasingly common condition in people of working age. The study also emphasises the need to develop better tools for clinical cognitive testing, which will enable physicians to assess and manage brain dysfunction early in MASLD.

Cognitive dysfunction in early experimental metabolic dysfunction-associated steatotic liver disease is associated with systemic inflammation and neuroinflammation



Kristoffer Kjærgaard,^{1,2,†} Anne Catrine Daugaard Mikkelsen,^{1,†} Anne M. Landau,^{3,4} Peter Lykke Eriksen,¹ Stephen Hamilton-Dutoit,⁵ Nils Erik Magnusson,⁶ Majken Borup Thomsen,^{3,4} Fenghua Chen,⁴ Hendrik Vilstrup,¹ Rajeshwar Prasad Mookerjee,^{1,7} Cecilie Bay-Richter,⁴ Karen Louise Thomsen^{1,7,*}

¹Department of Hepatology and Gastroenterology, Aarhus University Hospital, Denmark; ²Department of Emergency Medicine, Horsens Regional Hospital, Denmark; ³Department of Nuclear Medicine and PET, Aarhus University Hospital, Denmark; ⁴Translational Neuropsychiatry Unit, Department of Clinical Medicine, Aarhus University, Denmark; ⁵Department of Pathology, Aarhus University Hospital, Denmark; ⁶Medical Research Laboratory, Department of Endocrinology and Internal Medicine, Aarhus University Hospital, Denmark; ⁷Institute for Liver and Digestive Health, University College London, United Kingdom

JHEP Reports 2024. <https://doi.org/10.1016/j.jhepr.2023.100992>

Background & Aims: Cognitive dysfunction is an increasingly recognised manifestation of metabolic dysfunction-associated steatotic liver disease (MASLD), but the mechanistic link remains unclear. The aim of this study was to investigate the hypothesis that experimental MASLD leads to cognitive dysfunction via systemic inflammation and neuroinflammation.

Methods: Twenty male Sprague Dawley rats were randomised to a high-fat high-cholesterol (HFHC) diet to induce MASLD, or a standard diet (n = 10/group), for 16 weeks. Assessments included: MASLD severity (histology), neurobehaviour, inflammation (liver, plasma and cerebrospinal fluid), brain microglia and astrocyte activation, and synaptic density.

Results: The HFHC diet induced MASLD with extensive steatosis and lobular inflammation without fibrosis. Several plasma cytokines were elevated (CXCL1, IL-6, IL-17, MIP-1 α , MCP-1, IL-10; all $p < 0.05$) and correlated with increases in hepatic chemokine gene expression. Cerebrospinal fluid concentrations of CXCL1 were elevated ($p = 0.04$). In the prefrontal brain cortex, we observed a 19% increase in microglial activation confirmed by Iba1 immunohistochemistry ($p = 0.03$) and ³H-PK11195 autoradiography ($p < 0.01$). In parallel, synaptic density was reduced to 92%, assessed by ³H-UCB-J autoradiography ($p < 0.01$). MASLD animals exhibited impaired memory to previously encountered objects in the novel object recognition test ($p = 0.047$) and showed depression-like behaviour evidenced by increased immobility time ($p < 0.01$) and reduced swimming time ($p = 0.03$) in the forced swim test.

Conclusions: Experimental non-fibrotic MASLD, as a model to reflect the early stage of human disease, results in cognitive impairment and depression-like behaviour. This is associated with an inflammatory phenotype not only in the liver but also in the plasma and brain, which together with diminished synaptic density, provides a pathophysiological link between liver disease and cognitive dysfunction in MASLD.

Impact and implications: Cognitive dysfunction is an increasingly recognised comorbidity in patients with metabolic dysfunction-associated steatotic liver disease (MASLD), yet the underlying mechanisms remain unclear. This study provides evidence of impaired memory and depression-like symptoms in early experimental MASLD and indicates that hepatic inflammation may drive a systemic inflammatory response, resulting in neuroinflammation and reduced brain synaptic density. The evidence of impaired memory in MASLD and establishing its underlying pathophysiological link provides insights that could guide the development of potential new treatments for this increasingly common condition in people of working age. The study also emphasises the need to develop better tools for clinical cognitive testing, which will enable physicians to assess and manage brain dysfunction early in MASLD.

© 2023 The Authors. Published by Elsevier B.V. on behalf of European Association for the Study of the Liver (EASL). This is an open access article under the CC BY-NC-ND license (<http://creativecommons.org/licenses/by-nc-nd/4.0/>).

Keywords: Non-alcoholic fatty liver disease; non-alcoholic steatohepatitis; liver-brain axis; hepatic encephalopathy; neuroscience; cognitive dysfunction; neuroinflammation; systemic inflammation; synaptic density; metabolic dysfunction-associated steatotic liver disease; metabolic dysfunction-associated steatohepatitis. Received 10 May 2023; received in revised form 9 November 2023; accepted 8 December 2023; available online 21 December 2023

[†] Shared first authorship

* Corresponding author. Address: Department of Hepatology and Gastroenterology, Aarhus University Hospital, Palle Juul-Jensens Boulevard 99, C117, 8200 Aarhus N, Denmark.

E-mail address: karethom@rm.dk (K.L. Thomsen).

Introduction

Metabolic dysfunction-associated steatotic liver disease (MASLD), formerly known as non-alcoholic fatty liver disease (NAFLD), is estimated to affect up to 30% of the adult population worldwide.¹ MASLD is closely associated with the metabolic syndrome and has been linked with several extrahepatic complications including cognitive dysfunction.^{2,3} Given the large number of patients at risk, cognitive dysfunction in MASLD is an



increasing cause for concern, because it negatively affects patient quality of life and because it may already occur in the early stages of liver disease.^{4,5} However, the underlying mechanisms behind MASLD-related brain abnormalities have not been substantially investigated.⁵ The experimental evidence linking fatty liver with cognitive dysfunction is limited to a few animal studies in models that do not resemble the human phenotype of MASLD, or with sparse examination of behaviour and neurobiology.⁶

MASLD is accompanied by chronic low-grade systemic inflammation, even in its early stages before the development of hepatic necro-inflammatory changes and fibrosis.^{7–10} This systemic inflammation may affect the brain and induce neuroinflammation, which is believed to be important in the pathogenesis of neurodegenerative diseases associated with cognitive decline.^{11,12}

We hypothesised that, in rats with early non-fibrotic MASLD, a chain of events from hepatic and systemic inflammation to neuroinflammation results in behavioural cognitive disturbances and neurodegenerative changes. The present study aimed to test this hypothesis, in the hope of identifying possible future targets for therapy.

Materials and methods

Animal model

Male Sprague Dawley rats (body weight 298 ± 7 g; Taconic Biosciences, Köln, Germany) were housed in standard cages (GR1800; Tecniplast, Buguggiate, Italy) at 20 ± 2 °C with a 12-hour on/off light cycle. The animals were housed in pairs with free access to tap water and food. All animals were allowed to acclimatise for 1 week followed by randomisation to a standard diet or to a high-fat high-cholesterol (HFHC) diet at 10 weeks old.¹³ The standard diet consisted of 11% fat, 24% protein and 65% carbohydrates (3,227 kcal/kg) (1324, Altromin, Lage, Germany). The HFHC diet consisted of 39% fat (35% cocoa butter, 3% soybean oil, 2% cholesterol), 27% protein, 19% carbohydrates, and 0.5% cholic acid (4,057 kcal/kg) (D09052204, Research Diets, New Brunswick, NJ). All animals were weighed once per week throughout the experiment. The animals were monitored at least once daily and terminated if they met one of the following humane endpoints: weight loss $\geq 20\%$ of initial weight and lack of self-hygiene or activity. The protocol was approved by The Danish Animal Experiments Inspectorate (2016–15–0201–01105), and all experiments were performed according to the current law on animal experimentation and ethics. The animal experiments are reported in accordance with the ARRIVE guidelines.¹⁴

Study design

Twenty rats were randomised to a control group fed a standard diet or to a group fed a HFHC diet for 16 weeks to induce MASLD ($n = 10$ in each group). Starting 9 days before termination, all animals were assessed for cognitive function and for depression- and anxiety-like behaviour using validated behavioural tests. Following euthanasia, cerebrospinal fluid (CSF), blood samples, brain and liver tissue were collected for further analyses. The outcome measures were behavioural changes, measures of inflammation (liver, plasma and cerebrospinal fluid cytokines), brain microglia activation and astrogliosis, and brain synaptic density.

Neurobehavioural studies

The neurobehavioural studies were performed at the Translational Neuropsychiatry Unit, Aarhus University, over 9 consecutive days in the order listed below. The studies were performed in a designated experimental room, where the animals were acclimatised for 1 h before and after every test. All tests were recorded by video camera for subsequent analysis and were either analysed by automatic software or rated by an observer blinded to the intervention groups. The behavioural methods are described briefly below and in further detail in the supplementary materials and methods.

The conditioned fear paradigm (CFP) evaluated cognitive function.¹⁵ The test was performed in three phases: On day 1 (conditioning), a mild electric shock was used to condition a fear response to a spatial context and to a high-pitch noise stimulus. On day 2 (contextual test), the animals were observed for freezing behaviour (%) when reintroduced to the conditioned spatial context as a measure of hippocampal-dependent memory. On day 3 (cued test), the animals were observed for freezing behaviour (%) when reintroduced to the high-pitch noise in another spatial context as a measure of non-hippocampal-dependent memory.

The open field test (OFT) evaluated locomotion and anxiety-like behaviour. Moreover, the OFT served as habituation for the novel object recognition (NOR) test performed the following day. The animals were placed in a square arena to explore, and they were observed for distance travelled (cm) and time duration spent (%) in the periphery of the arena.

The NOR test evaluated recognition memory.¹⁶ The animals were placed in the OFT arena with two identical objects (encoding). Three hours later, the animals were reintroduced to the arena, with one of the two objects changed to a novel one (test). The NOR ratio (%) was calculated using time spent exploring the two objects ($(t_{\text{novel}} * 100) / (t_{\text{novel}} + t_{\text{old}})$).

The elevated plus maze (EPM) was performed to evaluate anxiety-like behaviour.¹⁷ The animals were placed in a maze shaped like a plus with two open arms and two closed arms. Time spent in the open arms was measured.

The forced swim test (FST) was performed to evaluate depression-like behaviour.¹⁸ The experiment was performed in two phases. As pre-test, the animals were placed in a clear plexiglass cylinder filled with water. Twenty-four hours later, the animals were tested in the same setting. The behaviour was scored manually every 5 s as either climbing, swimming, or immobility.¹⁹

Termination and tissue preparation

The procedures were performed between 9 am and 5 pm in a designated room at the Translational Neuropsychiatry Unit, Aarhus University. First, the animals were anaesthetised with an intraperitoneal injection of phenobarbital sodium (1 mg/kg; Fagron, Copenhagen, Denmark). Immediately after the loss of interdigital and corneal reflexes, CSF was extracted by percutaneous puncture into the cisterna magna, and blood was obtained from the retrobulbar plexus using heparinised capillary tubes. Next, the animals were decapitated, and the cerebrum was secured and split in two hemispheres. The right hemisphere was fixed in 10% formalin for immunohistochemistry. The left hemisphere was immersed in isopentane cooled to -30 °C with dry ice for 30 seconds and stored at -80 °C until processing for

autoradiography. The liver was removed surgically and weighed. Liver tissue samples were snap-frozen in liquid N₂ and stored at -80 °C for quantitative real-time PCR analysis. The remaining liver tissue was fixed in 10% formalin overnight followed by paraffin embedding for liver histology.

Blood and CSF analyses

Plasma was analysed for alanine aminotransferase, alkaline phosphatase, bilirubin, albumin, total cholesterol, HDL cholesterol, LDL cholesterol, triglyceride, and creatinine. Cytokines were analysed in plasma and CSF using a Luminex Immunoassay (Bio-plex Pro™ Rat Cytokine Assay, Bio-Rad Laboratories, Copenhagen, Denmark). Serum α₂-macroglobulin was evaluated using a specific rat ELISA (ICL Inc., Portland, US), performed according to manufacturer instructions.

Liver tissue analyses

Histopathology

Liver histology was evaluated by an experienced liver pathologist (SHD) blinded to the diet regimes. MASLD severity was scored on tissue sections stained with haematoxylin-eosin using the MASLD activity score, as previously described.²⁰ Fibrosis grade was evaluated with the Kleiner fibrosis score on sections stained with Sirius red.²⁰

mRNA measurements

The mRNA levels of two chemokines macrophage inflammatory protein-1α (MIP-1α, also known as CCL3) and fractalkine (CX3CL1) were analysed in liver tissue using quantitative real-time PCR. The mRNA levels of the genes of interest were normalised to a reference gene as 2^{-ΔCt} values. The results are reported as 2^{-ΔΔCt} values, which is the 2^{-ΔCt} of HFHC animals relative to the mean controls. The mRNA measurements are described in detail in the supplementary materials and methods.

Brain tissue analyses

Immunohistochemistry

The right hemisphere was embedded in 5% agar and sectioned at 65 μm thickness on a semi-automatic vibrating blade microtome (Leica VT1200, Leica Biosystems, Nussloch, Germany). All sections that included the prefrontal cortex and hippocampus were saved in 10% formalin. Twenty sections from the prefrontal cortex and from the hippocampus were selected by a systematic random sampling principle. Half of the sections were saved for analysis of microglia activation (stained for ionised calcium-binding adaptor molecule 1 [Iba1]) and the other half were saved for analysis of astrocyte density (stained for glial fibrillary acidic protein [GFAP]). Immunohistochemical analysis was performed in eight randomly chosen animals from each group.

Free-floating coronal sections were washed three times in Tris-buffered saline (TBS) (pH 7.4), immersed in endogenous peroxidase blocking solution for 30 min, and incubated in Target Retrieval solution at 85 °C for 30 min (Dako, Glostrup, Denmark). Tissue sections were incubated overnight at 4 °C in buffer (1% skimmed milk in TBS-T) with added anti-Iba1 (Abcam, Cambridge, UK, ab108539, dilution 1:500) or anti-GFAP (Dako, Glostrup, Denmark, ref Z0334, dilution 1:500). Sections were then washed three times with TBS and incubated in buffer (1% skimmed milk in TBS-T) with added secondary antibody for 2 h at room temperature. Sections were then washed three times for 10 min with TBS before and after the staining was visualised with

0.1% 3,3'-diaminobenzidine containing 0.3% H₂O₂ in TBS. Finally, sections were mounted on gelatine-coated slides, dehydrated with alcohol gradient, and cleared with xylene. GFAP sections were counterstained with 0.25% thionin solution (Thionin, Sigma T3387).

The stained sections were digitally scanned (NanoZoomer 2.0 HT, Hamamatsu, Shizuoka, Japan) and analysed using a machine learning plugin tool for ImageJ (FIJI Is Just ImageJ v1.53t; Trainable Weka Segmentation). The software was trained to classify Iba1 and GFAP staining against background and quantify the following outcomes (see supplementary materials and methods for details): number of microglia per area (/inch²) and mean perimeter of microglia (inches) as expression of microglia proliferation and microglia activation (Iba1), respectively, and percentage of area stained with GFAP (%) as expression of astrogliosis.²¹

Autoradiography

Autoradiography experiments were performed in the prefrontal cortex and hippocampus using the tracers ³H-PK11195 and ³H-UCB-J. ³H-PK11195 (Exp. 1) binds to mitochondrial translocator protein (TSPO), which is upregulated on activated microglia. ³H-UCB-J (Exp. 2) binds to synaptic vesicle glycoprotein 2A (SV2A), which is a transmembrane protein of presynaptic vesicles, and therefore ³H-UCB-J binding was used as a biomarker for synaptic density. The autoradiography experiments were performed in eight randomly chosen animals from each group, as previously described.²² The fresh-frozen left brain hemispheres were sliced into 20 μm thick coronal sections using a cryostat, mounted on poly-L-lysine coated slides (8 slices per slide, Thermo Scientific), and stored at -80 °C. Slices at the approximate levels of the prefrontal cortex (Bregma 3.7 mm) and dorsal hippocampus (Bregma -5.2 mm) were selected according to the stereotaxic coordinates of the rat brain atlas.²³ For each region and experiment, three consecutive slides were used; two slides were used to measure total binding and one slide was used to measure non-specific binding of the tracers. The slides were left to thaw at room temperature and pre-washed for 5 min in 50 mM Tris-HCl buffer (pH = 7.4). Slides for total binding were incubated with 1 nM ³H-PK11195 (specific activity 82.7 Ci/mmol; PerkinElmer, Exp. 1) or 3 nM ³H-UCB-J (specific activity 82 Ci/mmol; cat. no. NT1099, Novandi Chemistry AB, Sweden, Exp. 2) for 60 min in assay buffer, while slides for non-specific binding were incubated in the same concentration of radioligand but in the presence of the blocking reagents unlabeled PK11195 (20 μM, Exp. 1) or levetiracetam (600 μM, Exp. 2). All slides were post-washed in cold buffer two times for 1 min each, briefly dipped in Milli-Q water (4 °C), and dried under a stream of cold air. Slides with ³H-PK11195 were read for 6 h and slides with ³H-UCB-J were read for 2 h using BeaQuant v. 1.14 (ai4r, France). The images were analysed using the Beamage v.2.1.7 software. Specific binding of the tracers was obtained by subtracting the non-specific binding from the total binding. In-house standards with known radioactive ³H concentrations were included in every reading to generate a standard curve for calculation of the specific binding concentration (nM).

Statistical analyses

Statistical analyses were performed using Stata 17 (StataCorp LLC, TX, USA). Normality and homogeneity of variance were checked by QQ-plots and the F-test, respectively. If assumptions of normality and variance homogeneity were met, groups were

compared using the Student's *t* test and reported as mean ± SD. If not, the Mann-Whitney *U* test was used and data reported as median (IQR). Statistical analyses of plasma cytokines were adjusted for multiple comparisons using the Holm-Šidák method. Correlation analyses were performed using Pearson's correlation coefficient or Spearman's correlation coefficient in the case of skewed data. A *p* value below 0.05 was considered statistically significant in a two-tailed test.

Results

HFHC diet induced liver steatosis, lobular inflammation and metabolic changes

Animal characteristics and liver histology for the HFHC animals and controls are illustrated in Fig. 1 and summarised here. No animals were excluded based on humane endpoints. At termination, the body weight of the HFHC animals was slightly higher than that of control animals (Fig. 1A; mean 562 ± 54 g vs. 512 ± 36 g, *p* = 0.03). Mean food intake was lower in HFHC animals than controls (Fig. 1B; *p* <0.001). The liver weight (*p* <0.0001) and liver/body weight % (Fig. 1C; *p* <0.0001) were increased. The HFHC diet induced MASLD with grade 3 steatosis and a varying degree of inflammation (mean NAFLD activity score 4.1 ± 0.9), but not hepatocellular ballooning or fibrosis (Fig. 1D,E). The MASLD animals had hypercholesterolemia and elevated plasma LDL cholesterol levels (both *p* <0.01) as anticipated with a HFHC diet, but no change in plasma triglyceride levels compared with controls (Table 1).

MASLD animals exhibited chronic systemic inflammation which was associated with hepatic inflammation

The induction of MASLD was accompanied by a consistent increase in systemic pro-inflammatory cytokines (Fig. 2A). There was a two-fold increase in the cytokines C-X-C motif chemokine ligand 1 (CXCL1) and monocyte chemoattractant protein 1 (MCP-

1), whilst interleukin (IL)-6 and IL-17 were increased more than three-fold, and the chemokine MIP-1α was increased by more than 10 times compared with controls. Also, α₂-macroglobulin, an important acute phase reactant, tended to increase (median 18.5 vs. 13.5; *p* = 0.07). The rise in pro-inflammatory cytokines was accompanied by an increase in the anti-inflammatory cytokine IL-10 (Fig. 2A).

In the liver, gene expression of the chemokine MIP-1α was increased by 9-fold (*p* <0.0001) and CX3CL1 by 4-fold (*p* <0.01) in the MASLD animals (Fig. 2B). The pro-inflammatory plasma cytokines IL-6 (Spearman's ρ = 0.6, *p* = 0.005), MIP-1α (Spearman's ρ = 0.8, *p* <0.001) and MCP-1 (Spearman's ρ = 0.7, *p* <0.001) were strongly correlated with hepatic inflammation, as reflected by levels of MIP-1α expression in the liver (Fig. S3).

MASLD animals demonstrated neuroinflammation and loss of synaptic density

In the brains of MASLD animals, Iba1 staining revealed a decrease in the mean perimeter of microglia in the prefrontal cortex, an expression of microglia activation (Fig. 3E; *p* = 0.03). Moreover, there was a trend towards an increased percentage area stained positive for GFAP, a sign of astrogliosis (Fig. 3F; *p* = 0.13). There was no evidence of changed microglia perimeter or astrogliosis in the hippocampal regions, CA1 and dentate gyrus (Fig. 3E,F). The overall density of microglia was equal in all measured regions (data not shown).

The findings from immunohistochemical analyses were confirmed by ³H-PK11195 autoradiography showing a 19% increase in microglia activation in the prefrontal cortex of MASLD animals when compared with controls (Fig. 4C; *p* = 0.008), whereas there was no indication of increased microglia activation in the hippocampus. The chemokine CXCL1 was increased in the CSF of MASLD animals, supporting the presence of neuroinflammation in the prefrontal cortex (Fig. 2C; *p* = 0.04).

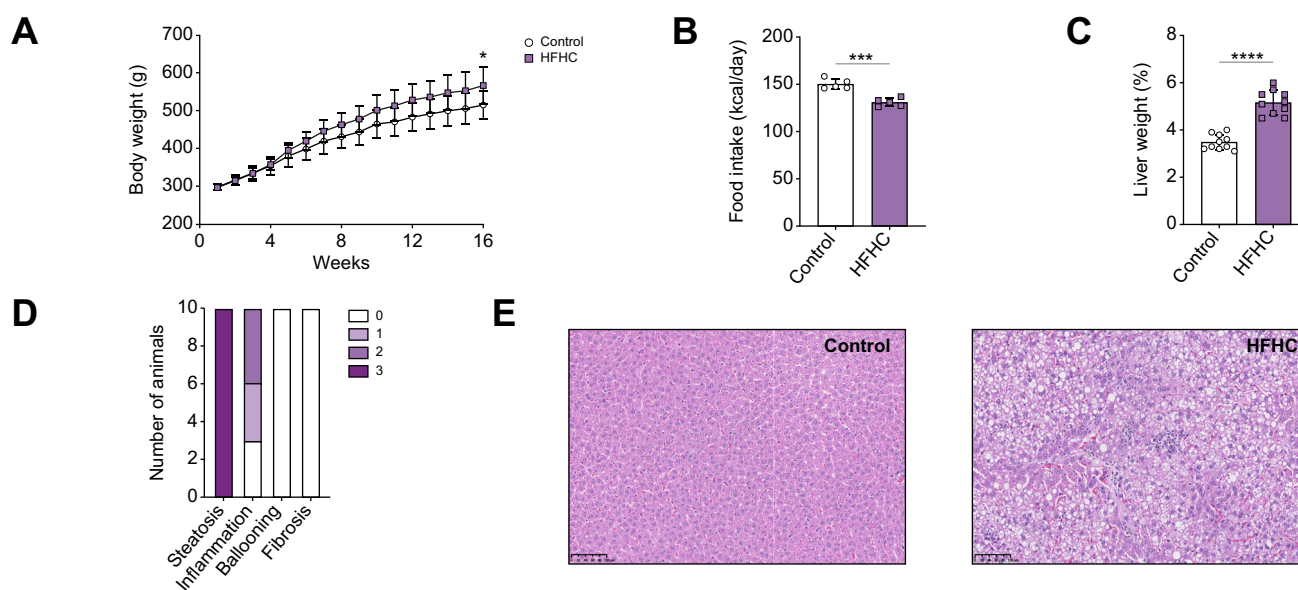


Fig. 1. Animal characteristics and liver histology. (A) Mean body weight (bars represent SD) during the course of the study in animals fed a HFHC diet (purple, square) or standard diet (white, circle) for 16 weeks. (B) Mean daily food intake (bars represent SD). (C) mean liver/body weight % at termination (bars represent SD). (D) Bar plot of the histological grading of liver tissue in HFHC animals. (E) Representative liver histology images displaying normal liver architecture in a control animal and severe steatosis and mild lobular inflammation in an HFHC animal. Number of animals = 10/group. Levels of significance: **p* <0.05; ****p* <0.001; *****p* <0.0001 (Student's *t* test). HFHC, high-fat high-cholesterol.

Table 1. Blood biochemistry.

Blood biochemistry	Control	HFHC
Total cholesterol (mmol/L)	2.02 ± 0.27	4.31 ± 1.53*
HDL cholesterol (mmol/L)	0.54 ± 0.07	0.47 ± 0.06
LDL cholesterol (mmol/L)	0.70 ± 0.24	3.19 ± 1.45*
Triglycerides (mmol/L)	1.71 ± 0.39	1.43 ± 0.53
ALT (U/L)	111 ± 84	118 ± 66
Albumin (g/L)	13.5 ± 1.1	12.7 ± 1.5
Glucose (mmol/L)	11.0 ± 4.2	10.7 ± 3.0
Creatinine (µmol/L)	33.3 ± 3.1	33.4 ± 7.4
α ₂ -macroglobulin (µg/L)	13.5 (10.3-26.2)	18.5 (12.0-105.0)

Blood biochemistry at termination in control animals and animals fed a HFHC diet for 16 weeks. Number of animals = 10 per group. Values are reported as mean ± SD or median (IQR). Level of significance: **p* < 0.05 (Student's *t* test). ALT, alanine aminotransferase; HDL, high-density lipoprotein; HFHC, high-fat high-cholesterol; LDL, low-density lipoprotein.

Furthermore, additional brain injury was demonstrated by ³H-UCB-J autoradiography, revealing diminished synaptic density in the prefrontal cortex of MASLD animals, which was reduced to 92% of that in controls (Fig. 4D; *p* = 0.005) but with no difference in the hippocampus.

MASLD animals displayed distinct neurobehavioural changes

MASLD animals exhibited impaired memory in the NOR test, as reflected by a decreased exploration of the novel object compared with control animals (Fig. 5A; mean NOR ratio 61% vs. 78%, *p* = 0.047) and no significant learning effect (one sample *t*-test compared with 50%, *p* = 0.1). Furthermore, MASLD animals spent more time being immobile (Fig. 5B; mean immobility 24% vs. 10%, *p* = 0.007) instead of swimming (Fig. 5B; mean swimming 25% vs. 34%, *p* = 0.03) in the FST, which is interpreted as a sign of despair and depression-like behaviour. We did not find any differences between MASLD and control animals in the OFT, EPM, or CFP (Figs 5C and S4). There was no correlation between the body weight of the animals at termination and the behavioural test results (Fig. S5).

Discussion

Using a well-established rodent model of early MASLD, we demonstrate the presence of cognitive dysfunction and show this

is associated with systemic inflammation and neuroinflammation in addition to diminished synaptic density in the prefrontal cortex. The demonstration that cognitive dysfunction is closely associated with systemic and neuroinflammation in a MASLD model is an important finding, which provides a pathological basis for the changes in brain function observed in early non-fibrotic stages of MASLD.

We used a comprehensive panel of established neuro-behavioural tests and showed that MASLD animals had impaired memory and exhibited depression-like behaviour. In the NOR test, MASLD animals had no preference for the novel object in contrast to controls who showed almost 80% preference for the novel object, indicating an impaired memory. In the FST, MASLD animals showed signs of despair by responding to the stress with immobility rather than swimming. Importantly, spontaneous locomotion assessed in the OFT was equal in MASLD animals and controls, suggesting the behavioural changes were not caused by physical limitations in the HFHC model. Moreover, none of the behavioural test results were correlated with body weight. However, we cannot exclude the possibility that obesity-related sarcopenia or altered body composition might affect the behavioural results, particularly during the FST. We also assessed cognitive function by the conditioned fear paradigm, and anxiety-like behaviour using the elevated plus maze and OFT, in which no differences were observed.

The induction of MASLD resulted in chronic systemic inflammation, as demonstrated by elevated plasma levels of several pro-inflammatory cytokines and the acute phase reactant α₂-macroglobulin.²⁴ Thus, the animal model exhibited a key feature of human MASLD with systemic inflammation, which is increasingly recognised as a driver of the disease and its extra-hepatic complications.²⁵ In particular, increased levels of IL-6, MIP-1α, and MCP-1 have been reported in human MASLD.^{8,9,26} IL-10, which is regarded as an anti-inflammatory cytokine, was also increased in the MASLD animals. Although results regarding IL-10 levels in MASLD are conflicting, similar observations have been reported for human MASLD and may be regarded as a compensatory anti-inflammatory response.^{27,28} The chemokine MIP-1α was elevated in the liver and highly increased in the blood of MASLD animals. Hepatic MIP-1α expression was posi-

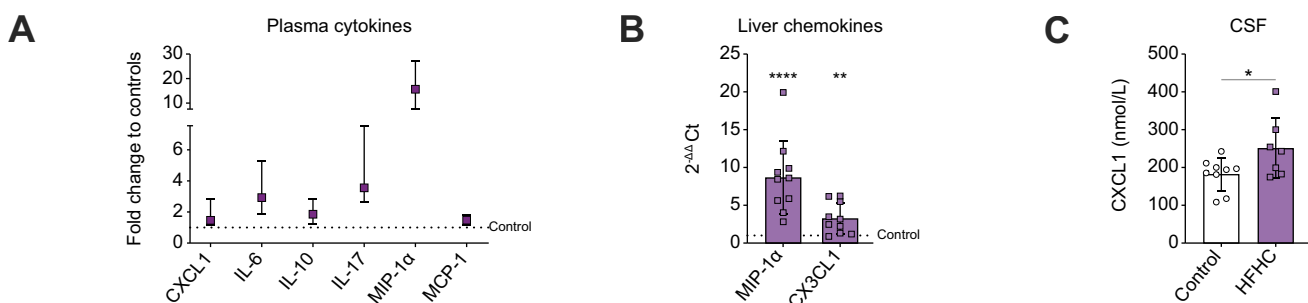


Fig. 2. Measurements of systemic inflammation, hepatic inflammation, and neuroinflammation. (A) Median plasma concentrations (bars represent IQR) of cytokines (CXCL1, IL-6, IL-10, IL-17, MIP-1α, MCP-1) in animals fed a HFHC diet for 16 weeks as fold changes relative to control animals. All cytokines displayed were elevated in the HFHC group compared with the control group (*p* < 0.05, Kruskal-Wallis test followed by Holm-Šidák multiple-comparisons *post hoc* test). (B) Mean liver gene expression (bars represent SD) of the chemokines MIP-1α and CX1CL3 in HFHC animals as fold changes relative to control animals. (C) Mean CSF concentrations (bars represent SD) of CXCL1 in HFHC (purple, square) and control (white, circle). Number of animals = 7-10/group. Levels of significance: **p* < 0.05; ***p* < 0.01; *****p* < 0.0001 (Student's *t* test). CSF, cerebrospinal fluid; HFHC, high-fat high-cholesterol.

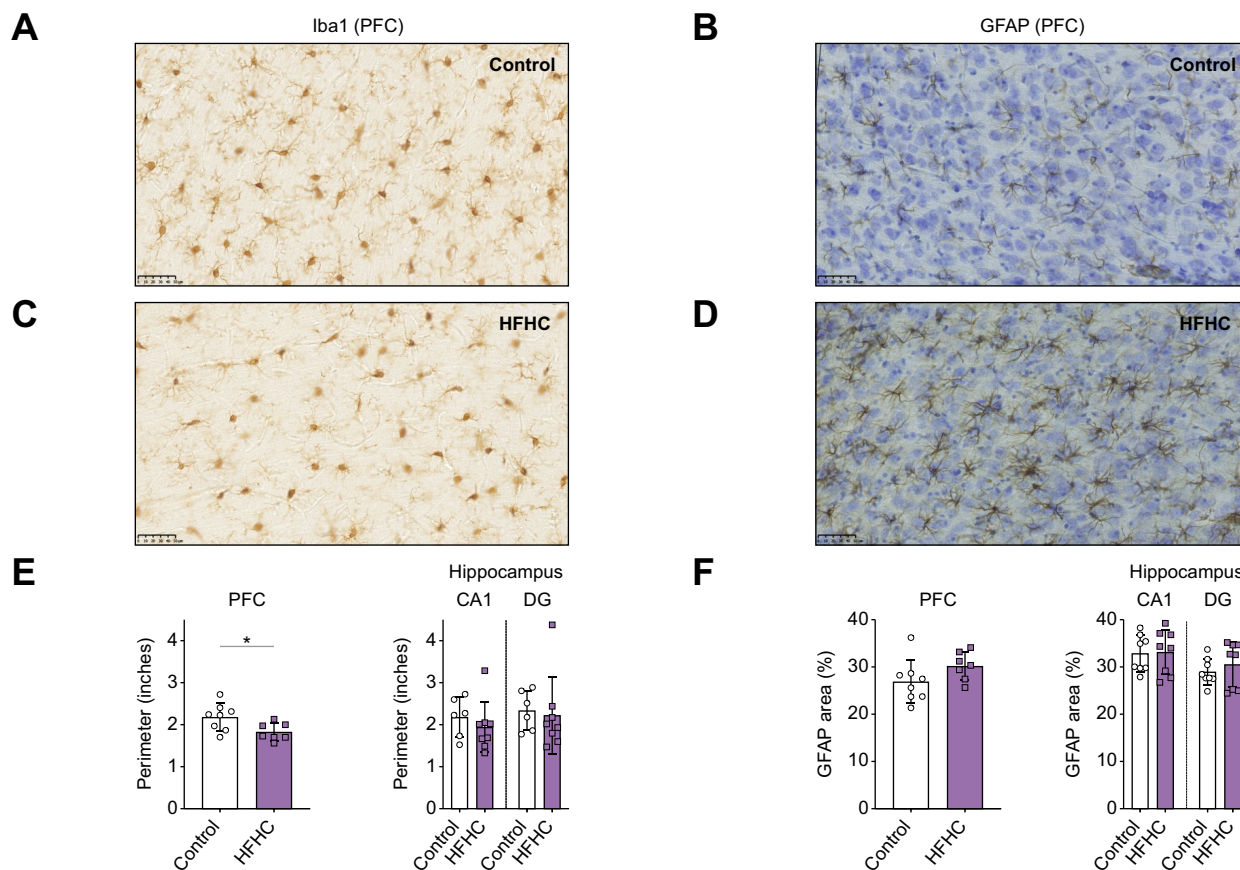


Fig. 3. Immunohistochemical staining for microglia and astrocyte morphology in the prefrontal cortex and hippocampus. (A-D) Representative images (20x) of microglia (Iba1) and astrocyte (GFAP) morphology in the PFC of control animals (A, B) and animals fed a HFHC diet for 16 weeks (A, C, E). There was an overall decreased ramification of microglia in HFHC animals reflecting increased microglia activation (E). Mean microglia perimeter (bars represent SD) was reduced in the PFC of HFHC animals (purple, square) compared to control animals (white, circle), but not in the hippocampus. (B, D) Mean GFAP area (bars represent SD) tended to increase in the PFC of HFHC animals reflective of astrogliosis, however, this difference was not significant (F). Number of animals = 7-8/group. Levels of significance: * $p < 0.05$ (Student's t test). GFAP, glial fibrillary acidic protein; HFHC, high-fat high-cholesterol; Iba1, ionised calcium-binding adaptor molecule 1; PFC, prefrontal cortex.

tively correlated with the pro-inflammatory plasma cytokines, IL-6, MIP-1 α and MCP-1. MIP-1 α is released by macrophages upon activation, including by hepatic Kupffer cells, which constitute the majority of macrophages in the human body. Accordingly, plasma MIP-1 α levels are associated with MASLD severity, and hepatic MIP-1 α is regarded as an important driver of systemic inflammation in MASLD.^{26,29}

Chronic systemic inflammation is believed to be an underlying cause of various neurodegenerative diseases, as it may induce brain immune activation and neuronal dysfunction in a number of ways; pro-inflammatory cytokines from the periphery do not cross the blood brain barrier (BBB) but can activate immune cells within the central nervous system through mechanisms such as direct action on vascular endothelial cells in the BBB, active transportation, or through receptor binding in circumventricular regions lacking the BBB.^{11,12} By similar mechanisms, neuroinflammation has been hypothesised to be a key factor for cognitive dysfunction in MASLD.^{5,30} We found evidence of microglia activation in the prefrontal cortex of MASLD animals confirmed by both autoradiography and immunohistochemical imaging methods. MASLD animals exhibited increased specific binding of [³H]PK11195, a tracer which labels the TSPO. TSPO is generally expressed at low levels in the normal brain but

increases greatly in microglia upon activation as well as in reactive astrocytes.³¹ For this reason, PK11195 binding is utilised as a marker of neuroinflammation in various diseases, where TSPO positron emission tomography imaging also allows for the assessment of neuroinflammation in humans.^{32,33} Complementary to the autoradiography findings, microglia morphology assessed with Iba1 immunohistochemistry showed reduced microglia perimeter in MASLD animals, further indicating increased microglia activation.³⁴ Moreover, there was a trend towards increased astrocyte proliferation in the prefrontal cortex assessed with immunohistochemical GFAP staining. It is a limitation that we were unable to measure brain cytokine levels given the lack of viable brain tissue after the autoradiography and immunohistochemistry analyses. However, in neuroinflammatory conditions, microglia activation is normally associated with a pro-inflammatory cytokine response, also noted in MASLD animal models.³⁵⁻³⁷ To this end, our observation of elevated CSF levels of CXCL1, a potent chemokine drawing in immune cells to sites of inflammation, further supports our contention that neuroinflammation occurs in this model.

Recent evidence suggests MASLD to be a driver of neurodegeneration with reports of reduced brain volume and increased risk of dementias, such as Alzheimer's disease, in patients with

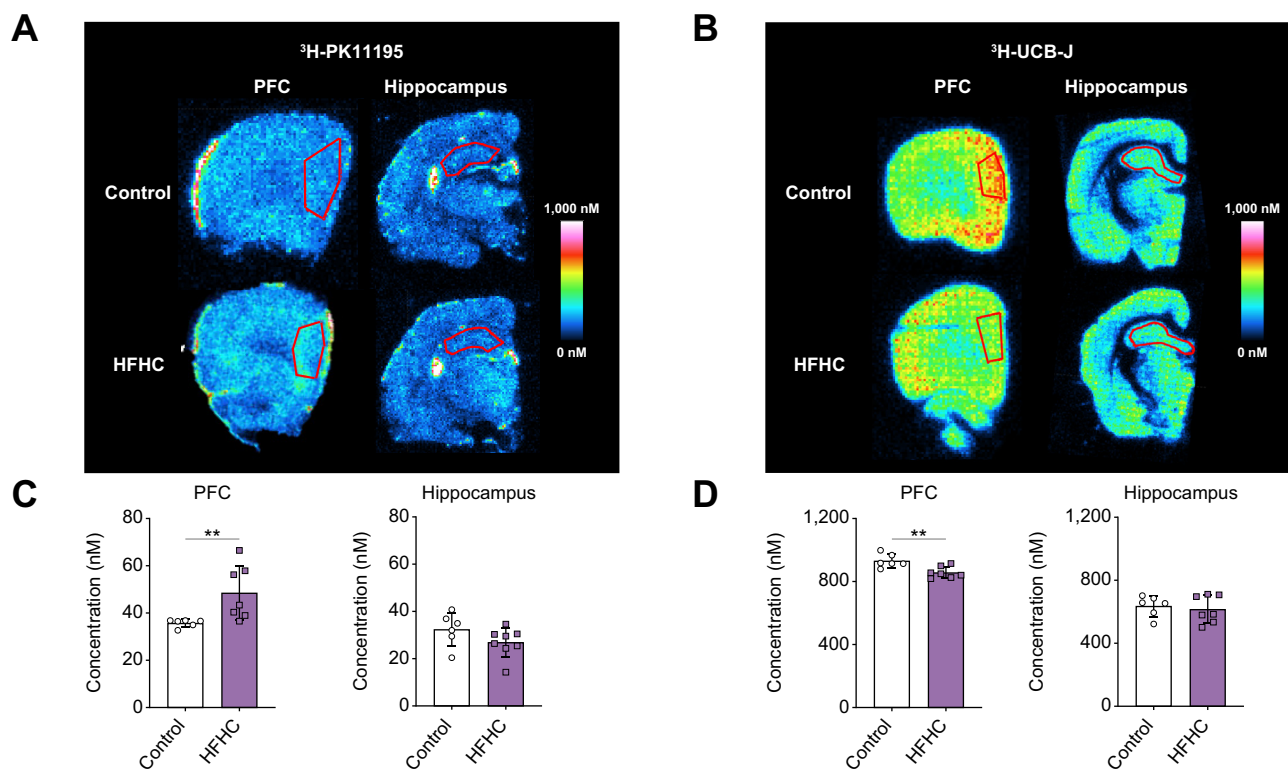


Fig. 4. Autoradiography imaging of microglia activation and synaptic density. (A,B) Autoradiography images displaying tracer binding of activated microglia (A; ³H-PK11195) and synaptic density (B; ³H-UCB-J) in the PFC and hippocampus of control animals and animals fed a HFHC diet for 16 weeks. (C) Median specific tracer binding concentration of ³H-PK11195 (bars represent IQR) and (D) mean specific tracer binding concentration of ³H-UCB-J (bars represent SD) in the PFC and hippocampus of control (white, circle) and HFHC animals (purple, square). (C) Specific binding concentration of ³H-PK11195 was increased in the PFC of HFHC animals reflecting microglia activation. (D) Specific binding concentration of ³H-UCB-J was decreased in the PFC of HFHC animals reflecting diminished synaptic density. There were no changes in the hippocampus. Number of animals = 6-7/group. Levels of significance: ***p* < 0.05 (Mann-Whitney *U* test [C] and Student's *t* test [D]). HFHC, high-fat high-cholesterol; PFC, prefrontal cortex.

MASLD.³⁸⁻⁴⁰ We found decreased ³H-UCB-J binding in the prefrontal cortex of the MASLD animals, indicative of neurodegeneration. The tracer binds to the SV2A protein, which is universally expressed in presynaptic terminals of neurons, and the decline in SV2A synaptic density is a pathological hallmark of neurodegenerative and psychiatric disease, supported by UCB-J *in vivo* imaging studies.⁴¹ In accordance with previous studies, we used ³H-UCB-J binding as a biomarker of synaptic density. It remains to be clarified as to what extent SV2A is capable of

representing the synapse as a whole when decreased.⁴¹ Our findings of neurodegeneration by molecular imaging in experimental MASLD are novel and are in line with previous experimental studies showing reduced brain-derived neurotrophic factor and increased neuronal cell death in the brains of MASLD animal models, reviewed in.⁶ It is unclear how this may be translated into human MASLD, since *in vivo* imaging studies of neurobiology in patients with MASLD are essentially lacking.⁵ However, in this study, we clearly show experimental MASLD to

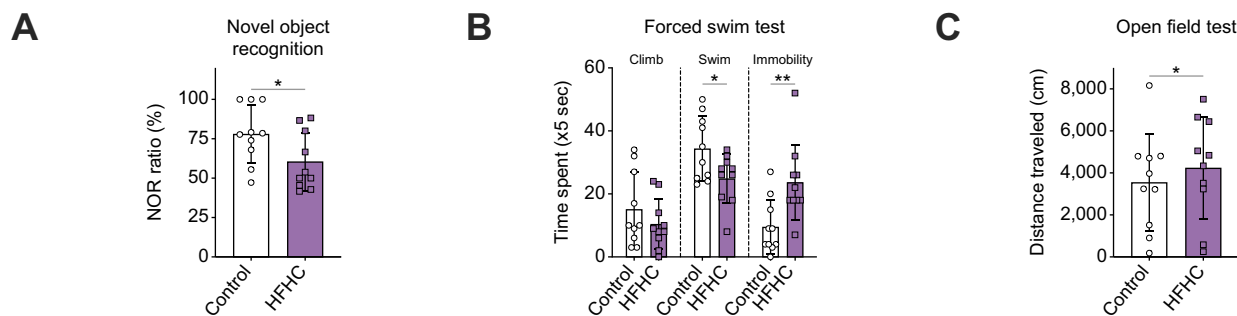


Fig. 5. Neurobehavioural test results. Neurobehavioural test results from control animals (white, circle) and animals fed a HFHC diet for 16 weeks (purple, square). (A) Mean NOR ratio (bars represent SD); HFHC animals exhibited impaired memory as shown by decreased NOR ratio compared with controls. (B) Mean time spent climbing, swimming or being immobile in the FST (bars represent SD); HFHC animals showed signs of depression-like behaviour by spending more time being immobile in the water instead of swimming. (C) Median distance travelled (bars represent IQR) in the OFT revealed no difference in locomotion between HFHC and control animals. Number of animals = 10/group. Levels of significance: **p* < 0.05; ***p* < 0.01 (Student's *t* test). FST, forced swim test; HFHC, high-fat high-cholesterol; NOR, novel object recognition; OFT, open field test.

be associated with microglia activation and diminished synaptic density in the prefrontal cortex, a brain region that is pivotal for higher cognitive function.⁴² We also assessed microglia activation and synaptic density in the hippocampus and found no changes. We chose to focus our investigations on the prefrontal cortex and hippocampus since synaptic connections between these two regions have been suggested to be required for normal cognitive function⁴³ and given previous studies reporting neurobiological changes in these regions in MASLD animal models.^{44–46} Optimal protein synthesis, c-Fos activation, and functional glial cells in the prefrontal cortex are required for normal performance in the NOR test.^{47,48} Furthermore, preserved function of the prefrontal cortex is essential in the FST.⁴⁹ Hence, the results of the behavioural tests in the present study are in accordance with the neurobiological findings in the prefrontal cortex. By contrast, the contextual part of the fear conditioning paradigm is known to be hippocampus-dependent,⁵⁰ and we found no changes in this test aligning with the lack of findings in this region in the neurobiological analyses. It is possible that other brain regions could be affected in MASLD animals besides those studied here, and this remains a question to be addressed in future studies.

Considering the growing number of clinical studies suggesting MASLD is independently associated with impaired cognitive function, the underlying mechanisms have so far not been investigated in detail.⁵ A major obstacle when studying the pathophysiology of MASLD cognitive dysfunction is isolating the direct effect of fatty liver from effects associated with the metabolic syndrome, including obesity, insulin resistance and atherosclerosis, and their individual contributions to brain dysfunction.⁵ Importantly, it was recently shown by Hadjihambi *et al.* that solitary elimination of hepatic steatosis through genetic knockout of the *MCT1* gene ameliorated neuroinflammation and anxiety-like behaviour in obese mice fed a high-fat diet.³⁷ These findings support the hypothesis investigated in the present study that there is a direct link between fatty liver and brain dysfunction. Another challenge is choosing a relevant model for investigating brain involvement in MASLD; such a model should encompass both hepatic steatosis with

inflammation and ideally features of the metabolic syndrome in order to mimic human MASLD. The 16-week HFHC diet for induction of MASLD resembles the human liver phenotype, and we demonstrated that the model exhibits both cognitive and neurobiological changes, making it suitable for preclinical studies of cognitive dysfunction in MASLD. A limitation to the HFHC model is the lack of peripheral insulin resistance and hypertriglyceridemia in mimicking the metabolic phenotype of patients with MASLD.⁵¹ However, our model does emphasise the direct effect of MASLD, since animals had severe steatosis and inflammation associated with cognitive disturbances that could not be attributed to brain insulin resistance or cardiovascular complications. Moreover, the strong association between hepatic and systemic inflammation, and the fact the MASLD animals were not grossly obese, indicates the fatty liver as the source of the systemic inflammation. Importantly, the model does not involve the use of neurotoxic agents like carbon tetrachloride, nor deprivation of nutrients that are essential for brain function, as is the case with methionine- and choline-deficient diets.⁶ This study aimed to characterise the animal model in the context of its cognitive function, but it is a limitation of the study that it was not designed to demonstrate a causative link between fatty liver and cognitive dysfunction. Our results should prompt further investigations into the mechanistic role of systemic inflammation in cognitive dysfunction in MASLD.⁵² Furthermore, numerous treatments targeting inflammatory pathways in MASLD are being tested, and future studies should investigate the potential of such drugs to reverse cognitive dysfunction along with the liver disease.

In conclusion, experimental MASLD leads to cognitive dysfunction in the form of impaired memory and depression-like behaviour at an early stage of liver disease. The cognitive dysfunction is associated with hepatic and systemic inflammation as well as neurobiological changes in the form of neuroinflammation and diminished synaptic density. Our results suggest a role for liver-derived systemic inflammation in the development of MASLD-related cognitive dysfunction, which may guide the design of future studies to identify potential targets for therapy.

Abbreviations

BBB, blood brain barrier; CFP, conditioned fear paradigm; CSF, cerebrospinal fluid; CXCL1, C-X-C motif ligand 1; EPM, elevated plus maze; FST, forced swim test; GFAP, glial fibrillary acidic protein; HFHC, high-fat high-cholesterol diet; Iba1, ionised calcium-binding adaptor molecule 1; IL, interleukin; MASLD, metabolic dysfunction-associated steatotic liver disease; MCP-1, monocyte chemoattractant protein 1; MIP-1 α , macrophage inflammatory protein-1 α ; NOR, novel object recognition; OFT, open field test; SVA2, synaptic vesicle glycoprotein 2A; TBS, Tris-buffered saline; TSPO, translocator protein.

Financial support

This work was supported by grants from the Novo Nordisk Foundation (NFF19OC0055039), Aarhus University Research Foundation, and the Foundation of Manufacturer Vilhelm Pedersen and Wife.

Conflicts of interest

RPM is a co-founder of Yaqrit Limited and has scientific collaborations with Cyberliver Limited and Hepyx Limited. The remaining authors have nothing to disclose.

Please refer to the accompanying ICMJE disclosure forms for further details.

Authors' contributions

KLT, RPM and CBR designed and conceived the study. KK and ACDM wrote the first draft. ACDM, KK and CBR performed the animal experiments and laboratory analyses. NEM, MBT, and CF assisted with laboratory analyses. SHD performed histological scoring. AML planned the autoradiography experiments. AML, PLE, HV, RPM, CBR, and KLT critically revised the manuscript for important intellectual content. All authors read and approved the final manuscript.

Data availability statement

The datasets generated and analysed for the current study are available from the corresponding author on reasonable request.

Acknowledgements

The authors would like to thank the staff at the Translational Neuropsychiatry Unit, Aarhus University, and the Department of Hepatology and Gastroenterology, Aarhus University Hospital, for helping with practical issues and experimental analyses. In particular, Marit Nyholm Nielsen has been of tremendous value, but we also would like to thank Mette Mejlbj Hansen, Pia Winther Andreasen and Julie Korgaard. Moreover, we would like to thank Karina Binda, Department of Nuclear Medicine and PET, Aarhus University Hospital, for assisting with autoradiography analyses.

Supplementary data

Supplementary data to this article can be found online at <https://doi.org/10.1016/j.jhepr.2023.100992>.

References

Author names in bold designate shared co-first authorship

- [1] Younossi ZM, Golabi P, Paik JM, et al. The global epidemiology of non-alcoholic fatty liver disease (NAFLD) and nonalcoholic steatohepatitis (NASH): a systematic review. *Hepatology* (Baltimore, Md) 2023;77(4):1335–1347.
- [2] Younossi ZM, Koenig AB, Abdelatif D, et al. Global epidemiology of nonalcoholic fatty liver disease—Meta-analytic assessment of prevalence, incidence, and outcomes. *Hepatology* (Baltimore, Md) 2016;64(1):73–84.
- [3] Targher G, Tilg H, Byrne CD. Non-alcoholic fatty liver disease: a multi-system disease requiring a multidisciplinary and holistic approach. *Lancet Gastroenterol Hepatol* 2021;6(7):578–588.
- [4] Younossi Z, Aggarwal P, Shrestha I, et al. The burden of non-alcoholic steatohepatitis: a systematic review of health-related quality of life and patient-reported outcomes. *JHEP Rep* 2022;4(9):100525.
- [5] Kjærsgaard K, Mikkelsen ACD, Wernberg CW, et al. Cognitive dysfunction in non-alcoholic fatty liver disease—current knowledge, mechanisms and perspectives. *J Clin Med* 2021;10(4).
- [6] Mikkelsen ACD, Kjærsgaard K, Mookerjee RP, et al. Non-alcoholic fatty liver disease: also a disease of the brain? A systematic review of the preclinical evidence. *Neurochem Res* 2022. <https://doi.org/10.1007/s11064-022-03551-x>.
- [7] Ndumele CE, Nasir K, Conceição RD, et al. Hepatic steatosis, obesity, and the metabolic syndrome are independently and additively associated with increased systemic inflammation. *Arteriosclerosis, Thromb Vasc Biol* 2011;31(8):1927–1932.
- [8] Haukeland JW, Damås JK, Konopski Z, et al. Systemic inflammation in nonalcoholic fatty liver disease is characterized by elevated levels of CCL2. *J Hepatol* 2006;44(6):1167–1174.
- [9] Fricker ZP, Pedley A, Massaro JM, et al. Liver fat is associated with markers of inflammation and oxidative stress in analysis of data from the framingham heart study. *Clin Gastroenterol Hepatol: official Clin Pract J Am Gastroenterological Assoc* 2019;17(6):1157–1164.e4.
- [10] **Nagata N, Chen G**, Xu L, et al. An update on the chemokine system in the development of NAFLD. *Medicina* (Kaunas) 2022;58(6).
- [11] Holmes C. Review: systemic inflammation and Alzheimer's disease. *Neuropathol Appl Neurobiol* 2013;39(1):51–68.
- [12] Glass CK, Saijo K, Winner B, et al. Mechanisms underlying inflammation in neurodegeneration. *Cell* 2010;140(6):918–934.
- [13] Thomsen KL, Gronbaek H, Glavind E, et al. Experimental nonalcoholic steatohepatitis compromises ureagenesis, an essential hepatic metabolic function. *Am J Physiol Gastrointest Liver Physiol* 2014;307(3):G295–G301.
- [14] Percie du Sert N, Hurst V, Ahluwalia A, et al. The ARRIVE guidelines 2.0: updated guidelines for reporting animal research. *Plos Biol* 2020;18(7):e3000410.
- [15] LeDoux JE. Emotion: clues from the brain. *Annu Rev Psychol* 1995;46:209–235.
- [16] Antunes M, Biala G. The novel object recognition memory: neurobiology, test procedure, and its modifications. *Cogn Process* 2012;13(2):93–110.
- [17] Rodgers RJ, Dalvi A. Anxiety, defence and the elevated plus-maze. *Neurosci biobehavioral Rev* 1997;21(6):801–810.
- [18] Cryan JF, Lucki I. Antidepressant-like behavioral effects mediated by 5-Hydroxytryptamine(2C) receptors. *J Pharmacol Exp Ther* 2000;295(3):1120–1126.
- [19] Cryan JF, Markou A, Lucki I. Assessing antidepressant activity in rodents: recent developments and future needs. *Trends Pharmacological Sciences* 2002;23(5):238–245.
- [20] Kleiner DE, Brunt EM, Van Natta M, et al. Design and validation of a histological scoring system for nonalcoholic fatty liver disease. *Hepatology* (Baltimore, Md) 2005;41(6):1313–1321.
- [21] Balzano T, Leone P, Ivaylova G, et al. Rifaximin prevents T-lymphocytes and macrophages infiltration in cerebellum and restores motor incoordination in rats with mild liver damage. *Biomedicines* 2021;9(8):1002.
- [22] Binda KH, Lillethorup TP, Real CC, et al. Exercise protects synaptic density in a rat model of Parkinson's disease. *Exp Neurol* 2021;342:113741.
- [23] Paxinos G, Watson C. The rat brain. In: *Stereotaxic coordinates*. San Diego: Academic Press; 1998.
- [24] van Vugt H, van Gool J, de Ridder L. Alpha 2 macroglobulin of the rat, an acute phase protein, mitigates the early course of endotoxin shock. *Br J Exp Pathol* 1986;67(3):313–319.
- [25] Adams LA, Anstee QM, Tilg H, Targher G. Non-alcoholic fatty liver disease and its relationship with cardiovascular disease and other extrahepatic diseases. *Gut* 2017;66(6):1138–1153.
- [26] Du Plessis J, Korf H, Van Pelt J, et al. Pro-inflammatory cytokines but not endotoxin-related parameters associate with disease severity in patients with NAFLD. *PloS one* 2016;11(12):e0166048.
- [27] **Duan Y, Pan X**, Luo J, et al. Association of inflammatory cytokines with non-alcoholic fatty liver disease. *Front Immunol* 2022;13:880298.
- [28] Cintra DE, Pauli JR, Araújo EP, et al. Interleukin-10 is a protective factor against diet-induced insulin resistance in liver. *J Hepatol* 2008;48(4):628–637.
- [29] Ma W. Expression of macrophage inflammatory protein-1 α in Kupffer cells following liver ischemia or reperfusion injury in rats. *World J Gastroenterol* 2006;12(24):3854.
- [30] Miller AA, Spencer SJ. Obesity and neuroinflammation: a pathway to cognitive impairment. *Brain Behav Immun* 2014;42:10–21.
- [31] Rupprecht R, Papadopoulos V, Rammes G, et al. Translocator protein (18 kDa) (TSPO) as a therapeutic target for neurological and psychiatric disorders. *Nat Rev Drug Discov* 2010;9(12):971–988.
- [32] Luo S, Kong X, Wu JR, et al. Neuroinflammation in acute hepatic encephalopathy rats: imaging and therapeutic effectiveness evaluation using (11)C-PK11195 and (18)F-DPA-714 micro-positron emission tomography. *Metab Brain Dis* 2018;33(5):1733–1742.
- [33] Varley J, Brooks DJ, Edison P. Imaging neuroinflammation in Alzheimer's disease and other dementias: recent advances and future directions. *Alzheimers Dement* 2015;11(9):1110–1120.
- [34] Wittekindt M, Kaddatz H, Joost S, et al. Different methods for evaluating microglial activation using anti-ionized calcium-binding adaptor protein-1 immunohistochemistry in the cuprizone model. *Cells* 2022;11(11).
- [35] Jena PK, Sheng L, Nguyen M, et al. Dysregulated bile acid receptor-mediated signaling and IL-17A induction are implicated in diet-associated hepatic health and cognitive function. *Biomark Res* 2020;8(1):59.
- [36] Kim DG, Krenz A, Toussaint LE, et al. Non-alcoholic fatty liver disease induces signs of Alzheimer's disease (AD) in wild-type mice and accelerates pathological signs of AD in an AD model. *J neuroinflammation* 2016;13:1.
- [37] Hadjihambi A, Konstantinou C, Klohs J, et al. Partial MCT1 inactivation protects against diet-induced non-alcoholic fatty liver disease and the associated brain dysfunction. *J Hepatol* 2023;78(1):180–190.
- [38] Weinstein G, Zelber-Sagi S, Preis SR, et al. Association of nonalcoholic fatty liver disease with lower brain volume in healthy middle-aged adults in the framingham study. *JAMA Neurol* 2018;75(1):97–104.
- [39] Shang Y, Widman L, Hagström H. Nonalcoholic fatty liver disease and risk of dementia: a population-based cohort study. *Neurology* 2022;99(6):e574–e582.
- [40] Cheon SY, Song J. Novel insights into non-alcoholic fatty liver disease and dementia: insulin resistance, hyperammonemia, gut dysbiosis, vascular impairment, and inflammation. *Cell Biosci* 2022;12(1):99.
- [41] Rossi R, Arjmand S, Bærentzen SL, et al. Synaptic vesicle glycoprotein 2A: features and functions. *Front Neurosci* 2022;16.
- [42] Miller EK. The prefrontal cortex and cognitive control. *Nat Rev Neurosci* 2000;1(1):59–65.
- [43] Wang C, Furlong TM, Stratton PG, et al. Hippocampus-prefrontal coupling regulates recognition memory for novelty discrimination. *J Neurosci* 2021;41(46):9617–9632.
- [44] Bocarsly ME, Fasolino M, Kane GA, et al. Obesity diminishes synaptic markers, alters microglial morphology, and impairs cognitive function. *Proc Natl Acad Sci USA* 2015;112(51):15731–15736.
- [45] Veniaminova E, Oplatchikova M, Bettendorff L, et al. Prefrontal cortex inflammation and liver pathologies accompany cognitive and motor deficits following Western diet consumption in non-obese female mice. *Life Sci* 2020;241:117163.
- [46] Pfohl M, DaSilva NA, Marques E, et al. Hepatoprotective and anti-inflammatory effects of a standardized pomegranate (*Punica granatum*) fruit extract in high fat diet-induced obese C57BL/6 mice. *Int J Food Sci Nutr* 2021;72(4):499–510.

- [47] **Tanimizu T, Kono K**, Kida S. Brain networks activated to form object recognition memory. *Brain Res Bull* 2018;141:27–34.
- [48] **Delcourte S, Bouloufa A**, Rovera R, et al. Chemogenetic activation of prefrontal astroglia enhances recognition memory performance in rat. *Biomed Pharmacother* 2023;166:115384.
- [49] Domingues K, Melleu FF, Lino De Oliveira C. Medial Prefrontal Cortex controlling the immobility of rats in the forced swimming test: a systematic review and meta-analysis. 2021.
- [50] Ratigan HC, Krishnan S, Smith S, et al. A thalamic-hippocampal CA1 signal for contextual fear memory suppression, extinction, and discrimination. *Nat Commun* 2023;14(1).
- [51] Lau JK, Zhang X, Yu J. Animal models of non-alcoholic fatty liver disease: current perspectives and recent advances. *J Pathol* 2017;241(1):36–44.
- [52] homsen KL, Eriksen PL, Kerbert AJC, De Chiara F, Jalan R, Vilstrup H. Role of ammonia in NAFLD. an unusual suspect. *JHEP Reports* July 2023;5(7):100780.